

Wetting of Argon on CO₂

Giampaolo Mistura, Francesco Ancilotto, Lorenzo Bruschi and Flavio Toigo
Istituto Nazionale per la Fisica della Materia and Dip.to di Fisica G. Galilei
Università di Padova, via Marzolo 8, 35131 Padova, Italy

We have studied the wetting transition of Ar adsorbed on solid CO₂ by means of high-precision adsorption isotherms measured with a quartz microbalance. We observe triple-point wetting. At variance with many theoretical studies based on a model adsorption potential, which predict for this system a genuine prewetting transition around 100K, we find that a detailed density-functional calculation employing a more realistic adsorption potential leads to triple-point wetting of Ar on CO₂, in good agreement with the experiment.

PACS numbers: 68.45.Gd;68.35.Rh

Recently, there has been a tremendous progress in the experimental investigations of wetting phenomena. For the first time, conclusive evidence for the first-order nature of the wetting transition, as originally predicted by Cahn [1] long time ago, together with its accompanying prewetting jumps away from the coexistence line, has been obtained in several different systems: quantum liquid films physisorbed on heavy alkali metals [2], complex organic liquids [3], near critical liquid mercury [4] and binary liquid crystal mixtures [5].

The first evidence of such a transition came however from mean-field numerical calculations of Ar adsorbed on solid CO₂ carried out by Ebner and Saam [6]. Several groups have subsequently studied this same model system with different numerical and analytical techniques and have essentially confirmed the original picture [7,8]. The most recent and accurate calculation predicts a prewetting transition of Ar on CO₂ around 105°K [8]. It is curious that despite such a keen theoretical interest, the wetting properties of Ar on solid CO₂ have never been investigated in a real experiment, to the best of our knowledge.

We have thus decided to study such a system with a quartz microbalance technique. This is a powerful quantitative probe in which the resonance frequency of an AT-cut crystal excited in its shear mode depends, among other things, on the mass of the film adsorbed on the metal electrodes of the quartz plate. To drive the crystal to its resonance frequency we have used an FM-technique described in detail elsewhere [9]. The quartz plate employed in this study has a fundamental resonance frequency of 5MHz with optically polished gold electrodes. The frequency shift caused by the adsorption of a monolayer of liquid Ar, $-\Delta f_m$, corresponds to approximately 6Hz. The resolution is of about $\pm 0.05Hz$ with an excitation power dissipated onto the crystal of less than 50nW. The AT-plate is housed in a double-wall OFHC copper cell (see Fig. (1)) to reduce thermal gradients. The entire set-up is attached to the cold flange of an homemade liquid nitrogen cryostat. The maximum temperature difference between the top and bottom parts inside the inner copper cell is estimated to be less than 1μK. The temperature stability is better than 0.5mK. The Ar gas is admitted into the cell through a thin capillary very well

heat sunk to the base of the copper cells. A copper foil, glued to the bottom of the inner cell, faces the extremity of the Ar capillary to shield the quartz crystal from the incoming warm vapor which is slowly admitted into the cell during the measurements.

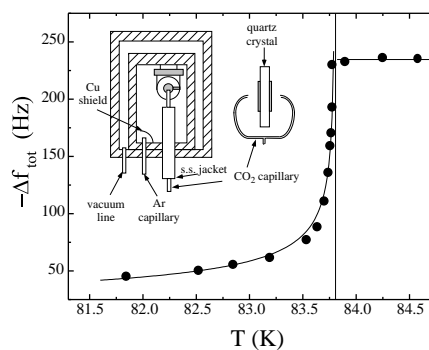


FIG. 1. Total film thickness of Ar on CO₂ as a function of T. The vertical line indicates T_t. Inset: schematic drawing of the sample cell housing the quartz crystal and enlargement of the CO₂ evaporator.

The CO₂ substrate is evaporated at low temperature ($\approx 85^\circ K$) directly onto the two opposite gold electrodes of the quartz crystal through a different capillary also connected to the gas system. At the temperature of evaporation, the vapor pressure of CO₂ is $\approx 1\mu Torr$. CO₂ is thus admitted to the cell through a copper capillary mounted inside a stainless steel tube, soldered to the base of the inner cell (see Fig. (1)). The copper capillary, wrapped by a resistive wire, is soldered to the opposite end of the s.s. tube. In this way, it is possible to heat up the CO₂ capillary to a temperature much higher than that of the quartz and thus avoid its blocking during the evaporation. The capillary ends in two curved pieces placed in front of the two faces of the quartz crystal (see Fig. (1)). By slowly admitting high-purity CO₂ gas through this heated capillary it is then possible to evaporate CO₂ films with a mass corresponding to thicknesses ranging from 100 to 1000 layers over a period of about 2-10 minutes.

The wetting transition of Ar on CO₂ has been experimentally investigated by means of adsorption isotherms.

These are determined by slowly admitting small amounts of high-purity Ar gas into the sample cell, kept at a constant temperature. The resonance frequency and the pressure inside the sample cell are continuously monitored with a personal computer. Saturation is reached when P remains unchanged after further admission of a small amount of gas.

Fig.(1) shows the results of a set of adsorption isotherms taken across the bulk triple-point of Ar on gold preplated with more than 100 equivalent layers of CO_2 . The vertical axis reports the total frequency shift $-\Delta f_{tot}$ measured at pressures between vacuum and coexistence vapor pressure and corrected by vapor contributions in the standard way [2,9]. Since the film thickness is proportional to the corrected frequency shift, the maximum thickness of the Ar liquid films is found to remain practically constant over the investigated temperature range, as the horizontal line clearly shows. Finally, on bare gold $-\Delta f_{tot}$ is only 5% smaller than on this CO_2 plating. This difference is likely to be caused by the rough CO_2 substrate evaporated at low temperature which makes the active surface area of the microbalance larger than that of the gold electrodes. However, such a small effect indicates that the roughness of this CO_2 substrate does not play a significant role in our measurements.

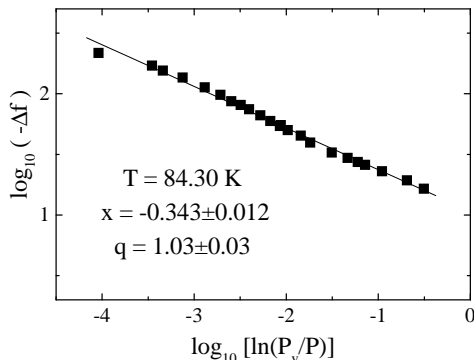


FIG. 2. Determination of the growth exponent x of Ar on CO_2

In the solid phase, $-\Delta f_{tot}$ is found to grow continuously as T approaches T_t . We have also taken isotherms on gold preplated with different CO_2 coverages ranging from 200 to about 1000 equivalent layers. These measurements agree well with the results of Fig. (1) apart from an increased frequency noise and a larger value of $-\Delta f_{tot}$ observed at the higher coverages, probably caused by rougher surfaces. Similar behavior, seen in all physisorbed systems characterized by strong substrates, is typical of triple-point wetting. We have thus fitted the points below T_t in Fig. (1) according to the power law expected for this phenomenon [10], $-\Delta f_{tot} = [AT(T_t - T)^x]$, where $A = \frac{-\Delta f_m^3}{\alpha_{Ar-CO_2}} \left[\left(\frac{1}{P_v} \frac{dP_v}{dT} \right)_{sol} - \left(\frac{1}{P_v} \frac{dP_v}{dT} \right)_{liq} \right]$,

α_{Ar-CO_2} being the adsorbate-substrate Hamacker constant, $-\Delta f_m = 6Hz$ the frequency shift corresponding to the adsorption of an Ar monolayer and $x = -1/3$ for van der Waals interactions. The results of the nonlinear least square fit are: $T_t = 83.80 \pm 0.02K$, in very good agreement with the tabulated bulk triple-point of Ar, $T_t = 83.806 K$, $x = -0.337 \pm 0.008$ and $A = 1.5 \times 10^{-5} K^{-2} Hz^{-3}$. We have also analyzed the film growth of the isotherms taken above T_t . Under the assumption of complete wetting at coexistence, the film thickness is predicted to grow according to the Frenkel-Halsey-Hill relation [10], $-\Delta f = -\Delta f_m \left[\frac{T}{\alpha_{Ar-CO_2}} \ln \left(\frac{P_v}{P} \right) \right]^{-1/3}$ where the exponent $-1/3$ reflects again the van der Waals nature of the interaction. In Fig.(2) the quantity $\log_{10}(-\Delta f)$ is plotted as a function of $\log_{10}[\ln(P_v/P)]$. As expected, near saturation the experimental points lie on a reasonable straight line. The slope of the linear fit is -0.343 ± 0.012 , in good agreement with the FHH equation. From the intercept q we have also estimated a value for $\alpha_{Ar-CO_2} = 19000 K \text{\AA}^3 \pm 20\%$, in reasonable agreement with the van der Waals tail used by Ebner and Saam [6]. A similar value, although affected by a larger error, has been deduced from the parameter A of the previous fit.

Motivated by these experimental findings, which are in disagreement with the previous theoretical predictions of a prewetting transition in this system, we have re-examined the basis for such predictions and found that they are flawed in one of their basic premises, i.e. in the form of the fluid-substrate interaction potential. Common to these theoretical studies is in fact the assumption, as made by Ebner and Saam [6], that the Ar- CO_2 interaction is represented by a (12-6) Lennard-Jones potential whose hard-core diameter and well depth are deduced, through simple combining rules [11], from those of Ar-Ar and CO_2 - CO_2 . An integration of the (12-6) potential over a continuum of CO_2 substrate atoms produces a (9-3) adsorption potential, hereafter called Ebner-Saam (ES) potential, which has been used in almost all the theoretical calculations published so far [7,8].

By comparing this potential with a more realistic one, which we compute by explicitly taking into account the structure of the CO_2 substrate, as shown below, we find that the ES potential underestimates the real interaction between Ar atoms and solid CO_2 . Our density functional calculations encompassing the newly calculated adsorption potential support the experimental evidence reported above of triple-point wetting.

In our density functional calculation the free energy of the fluid is written in term of the density $\rho(\vec{r})$ of the fluid as:

$$F[\rho] = F_{HS}[\rho] + \int \rho(\vec{r}) V_s(\vec{r}) d\vec{r} + \frac{1}{2} \int \int \rho(\vec{r}) \rho(\vec{r}') u_a(|\vec{r} - \vec{r}'|) d\vec{r} d\vec{r}' \quad (1)$$

Here F_{HS} is a non-local free-energy functional for the

inhomogeneous hard-sphere reference system, $V_s(\vec{r})$ is the external adsorption potential due to the surface, while the third term is the usual mean-field approximation for the attractive part of the fluid-fluid intermolecular potential, u_a . F_{HS} is evaluated according to the theory of Ref. [12], which has been found to give an accurate description of inhomogeneous fluids even in situations where strong density variations occur, as in the presence of hard walls or strongly attractive substrates. Following Ref. [8,13] we describe the attractive part of the interparticle potential as an effective interaction

$$u_a(r) = 0 \quad , \quad r \leq \lambda^{1/6}\sigma$$

$$= 4\epsilon\{\lambda(\sigma/r)^{12} - (\sigma/r)^6\} \quad , \quad r > \lambda^{1/6}\sigma \quad (2)$$

We determine the free parameters λ and σ (the HS diameter) for each temperature by requiring that the experimental values of liquid and vapor densities at coexistence, ρ_l and ρ_v , are reproduced for the bulk fluid. In order to correctly describe the bulk phase diagram, it is important to verify that the thermodynamic equilibrium conditions are satisfied. This is done by means of a Maxwell (equal-area) construction in the $P - \rho$ plane.

CO₂ has a unique crystalline phase at low temperature and pressure [14]. Thin solid films of CO₂ are known to have crystalline structure [15] when grown at $T > 80^\circ K$ and in a wide range of growth rates, including those realized in our experiment. Moreover, it is found experimentally [15] that the exposed surface is almost invariably the (001) face of the crystal.

Accurate *ab initio* potentials are available [16], which describe the interaction between a CO₂ molecule and an Ar atom. Due to the nature of the bonding in CO₂ solid (van der Waals + electrostatic forces) no appreciable electron charge redistribution is expected between the molecules in the solid. We may thus calculate the total Ar-surface potential by directly summing the two-body interactions between an Ar atom and the CO₂ molecules in the crystal, assuming that the exposed surface is the ideal (001). The resulting potential energy surface as a function of the lateral position of the Ar atom exhibits large variations, with differences in binding energies for different adsorption sites of more than $500^\circ K$. In particular, in the $c(2 \times 2)$ surface unit cell of the clean (001) surface there are two (non-equivalent) adsorption sites with very large ($\sim 1000^\circ K$) binding energies. We then make the assumption that at the low temperatures investigated here, at least one Ar monolayer is adsorbed on these sites as a solid-like layer. We determine the Ar equilibrium positions by energy optimization, neglecting however any relaxation of the CO₂ surface. The structure of the adsorbed monolayer is shown in the upper part of Fig. (3). We finally average laterally the interaction potential between Ar and this Ar-preplated surface, to get the adsorption potential $V_s(z)$ to be used in our calculations (z is the coordinate normal to the surface plane). This is shown in the lower part of Fig. (3), where it is compared with the original ES potential. The origin of

the z axis is taken at the position of the outmost layer of C atoms in the case of the ES potential, while it is taken at the position of the solid Ar monolayer for our calculated $V_s(z)$. Note that the net adatom-surface potential is deeper than the ES potential even if the CO₂ surface is screened by the solid Ar layer. This is a consequence of the large corrugation of the CO₂ surface: the structure and orientation of the CO₂ molecules on the surface plane (see Fig.(3)) allow the Ar monolayer to be easily accommodated but still leaving space for additional Ar atoms to come close to the surface, thus experiencing the attractive part of the interaction.

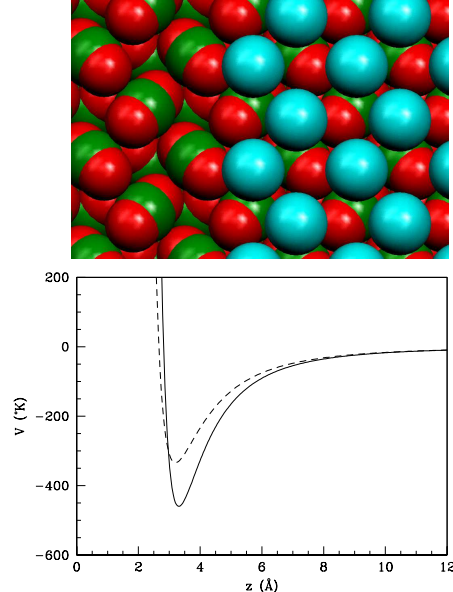


FIG. 3. Upper part: top view of the CO₂ surface. The left part shows the clean, ideal surface: C atoms and O atoms are represented by the green and red balls respectively. The right part shows the surface covered with a monolayer of Ar atoms (blue balls), in the positions as explained in the text. Lower part: fluid-substrate laterally-averaged potential. The dashed line shows the ES potential, while the solid line is our calculated potential. See text for the definition of the $z = 0$ planes.

The equilibrium Ar density profile $\rho(z)$ is determined by direct minimization of the functional (1) with respect to density variations. In practice we fix the coverage $\Gamma = \int dz \rho(z)$ and solve iteratively the Euler equation $\mu = \delta F / \delta \rho(z)$, where the value of the chemical potential μ is fixed by Γ .

We have considered two isotherms, one at $T = 105^\circ K$, which has been studied in most detail in Refs. [8], and one at $T = 85^\circ K$, i.e. just above the triple point T_t . We report our results in Fig. (4), where the chemical potential, measured with respect to its value at coexistence, is plotted vs. the film thickness. The latter is expressed in nominal layers $l = \rho_l^{-2/3} \int_0^\infty [\rho(z) - \rho_v] dz$. The dots show the calculated points at $T = 105^\circ K$, where one observes a smooth increase of coverage with chemical potential as

the saturated liquid is approached from below. At variance with the results of Ref. [8], we do not observe any sign of a prewetting transition. We show for comparison in the same figure the results obtained, at the same temperature, by using the ES potential (triangles). The large oscillation with positive values of μ is representative of a thin film-thick film prewetting transition, in agreement with previous calculations using the same potential [6–8]. A jump in the coverage from $l \sim 0.8$ to $l \sim 6$ can be readily obtained from our data by means of a Maxwell equal-area construction (dashed line).

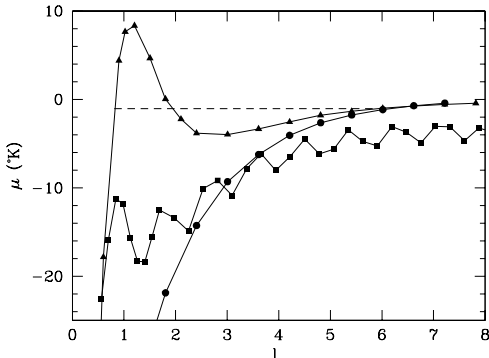


FIG. 4. Calculated adsorption isotherms of Ar in the fluid phase. Triangles: $T = 105^\circ K$, as calculated with the ES potential. Dots: $T = 105^\circ K$, with the new potential. Squares: $T = 85^\circ K$, with the new potential.

The calculated points at $T = 85^\circ K$ are shown with squares. A sequence of oscillations occurs in this case, whose period is one nominal layer, corresponding to the condensation of successive Ar monolayers (“layering” transitions).

Additional theoretical support to triple-point wetting of Ar on CO_2 can be obtained from a simple but surprisingly accurate heuristic model [17] where the energy cost of forming a thick film is compared with the benefit due to the gas-surface attractive interaction,

$$(\rho_l - \rho_v) \int_{z_0}^{\infty} V_s(z) dz = -2\gamma \quad (3)$$

Here ρ_l and ρ_v are the densities of the adsorbate liquid and vapor at coexistence, γ is the surface tension of the liquid and z_0 is the equilibrium distance of the potential V_s . By using for V_s our calculated potential and the experimental values for $\rho_l(T)$, $\rho_v(T)$ and $\gamma(T)$, we find that Eq.(3) is satisfied at $T_W = 1.03 T_t$.

In conclusions, our experimental results suggest triple-point wetting of Ar on solid CO_2 , in contrast to the many previous theoretical investigations. To clarify this finding, we have implemented density functional calculations. A crucial ingredient is a realistic form for the fluid-surface potential, which is obtained by explicitly considering the microscopic structure of the surface of solid CO_2 and the anisotropy of the Ar- CO_2 interaction. The result is a stronger potential than originally estimated by Ebner

and Saam by summing isotropic Ar- CO_2 LJ interactions over a continuum substrate. The increased binding of the surface changes dramatically the Ar growth mode, which now results in a continuous (layer-by-layer) film growth rather than exhibiting a prewetting transition. The results of our calculations are consistent with a wetting temperature close to the triple point, in agreement with our quartz microbalance measurements.

We thank Stefano Sitran and Gilberto Schiavon for the preparation of the quartz crystals used in this work.

-
- [1] J.W.Cahn, *J.Chem.Phys.* **66**, 3667 (1977).
 - [2] P. Taborek and J.E. Rutledge, *Phys. Rev. Lett.* **68**, 2184 (1992); G.B.Hess, M.J.Sabatini and M.H.W.Chan, *ibid.* **78**, 1793 (1997); D. Ross, P. Taborek and J.E. Rutledge, to be published in *Phys. Rev. B*; G. Mistura, H.C. Lee and M.H.W. Chan, *J. Low Temp. Phys.* **96**, 1 (1994).
 - [3] H.Kellay, D.Bonn and J.Meunier, *Phys. Rev. Lett.* **71**, 2607 (1993).
 - [4] V.F.Kozhevnikov, D.I.Arnold, S.P.Naurzakov and M.E. Fisher, *Phys. Rev. Lett.* **78**, 1735 (1997).
 - [5] R.Lucht and C.Bahr, *Phys. Rev. Lett.* **78**, 3487 (1997).
 - [6] C.Ebner and W.F.Saam, *Phys. Rev. Lett.* **38**, 1486 (1977).
 - [7] See e.g., R.Evans and P.Tarazona, *Phys. Rev. A* **28**, 1864 (1983); P.Tarazona and R.Evans, *Mol. Phys.* **48**, 799 (1983); E.Bruno, C.Caccamo and P.Tarazona, *Phys. Rev. A* **35**, 1210 (1987); J.E.Finn and P.A.Monson, *ibid.* **39**, 6402 (1989); *ibid.* **42**, 2458 (1990); S.Sokolowsky and J.Fischer, *ibid.* **41**, 6866 (1990); E.Velasco and P.Tarazona, *ibid.* **42**, 2454 (1990), and references therein.
 - [8] Y. Fan and P.A. Monson, *J. Chem. Phys.* **99**, 6897 (1993), and references therein.
 - [9] L. Bruschi, G. Delfitto and G. Mistura, to be published in *Rev. Sci. Instrum.*
 - [10] J.Krim, J.G.Dash, and J.Suzanne, *Phys.Rev.Lett.* **52**, 640 (1984); L.Bruschi, G.Torzo, and M.H.W.Chan, *Europhys. Lett.* **6**, 541 (1988).
 - [11] W.A.Steele, *Surf. Sci.* **36**, 317 (1973).
 - [12] E.Kierlik and M.L.Rosinberg, *Phys. Rev. A* **42**, 3382 (1990).
 - [13] E.Velasco and P.Tarazona, *J.Chem.Phys.* **91**, 7916 (1989).
 - [14] W.H.Keesom and J.W.L.Kohler, *Physica* **1**, 655 (1934); A.E.Curzon, *Physica* **59**, 733 (1972).
 - [15] M.J.Weida, J.M.Sperhac and D.J.Nesbitt, *J. Chem. Phys.* **105**, 749 (1996), and references therein.
 - [16] P.J.Marshall et al., *J. Chem. Phys.* **104**, 6569 (1996).
 - [17] E.Cheng, M.W.Cole, W.F.Saam and J.Treiner, *Phys. Rev. B* **48**, 18214 (1993).